Inorg. Chem. **2003**, *42*, 6886–6897

New Luminescent Cyclometalated Iridium(III) Diimine Complexes as Biological Labeling Reagents

Kenneth Kam-Wing Lo,*,† Chi-Keung Chung,† Terence Kwok-Ming Lee,† Lok-Hei Lui,† Keith Hing-Kit Tsang,† and Nianyong Zhu‡

Department of Biology and Chemistry, City University of Hong Kong, Tat Chee Avenue, Kowloon, Hong Kong, P. R. China, and Department of Chemistry, The University of Hong Kong, Pokfulam Road, Hong Kong, P. R. China

Received June 19, 2003

We report the synthesis, characterization, and photophysical and electrochemical properties of thirty luminescent cyclometalated iridium(III) diimine complexes $[Ir(N\text{-}C)_2(N\text{-}N)](PF_6)$ (HN-C = 2-phenylpyridine, Hppy; 2-(4-methylphenyl)-pyridine, Hmppy; 3-methyl-1-phenylpyrazole, Hmppz; 7,8-benzoquinoline, Hbzq; 2-phenylquinoline, Hpq; N-N = 4-amino-2,2′-bipyridine, bpy-NH_2; 4-isothiocyanato-2,2′-bipyridine, bpy-ITC; 4-iodoacetamido-2,2′-bipyridine, bpy-IAA; 5-amino-1,10-phenanthroline, phen-NH_2; 5-isothiocyanato-1,10-phenanthroline, phen-ITC; 5-iodoacetamido-1,-10-phenanthroline, phen-IAA). The X-ray crystal structure of $[Ir(mppz)_2(bpy\text{-}NH_2)](PF_6)$ has also been investigated. Upon irradiation, all the complexes display intense and long-lived luminescence under ambient conditions and in 77-K glass. On the basis of the photophysical and electrochemical data, the emission of most of these complexes is assigned to an excited state of predominantly triplet metal-to-ligand charge-transfer (^{3}MLCT) ($d\pi(Ir) \rightarrow \pi^*(N\text{-}N)$) character. In some cases, triplet intraligand (^{3}IL) ($\pi \rightarrow \pi^*$)(N-N or N-C$^-$) excited states have also been identified. In view of the specific reactivity of the isothiocyanate and iodoacetamide moieties toward the primary amine and sulfhydryl groups, respectively, we have labeled various biological molecules with a selection of these luminescent iridium(III) complexes. The photophysical properties of the luminescent conjugates have been investigated. In addition, a heterogeneous assay for digoxin has also been designed on the basis of the recognition of biotinylated anti-digoxin by avidin labeled with one of the luminescent iridium(III) complexes.

Introduction

Bioconjugation is an important procedure because it can provide new and useful properties to biological molecules for detection purposes and for gaining insights in biological recognition.[1] Traditionally, labeling of biomolecules for DNA sequencing, hybridization studies, and immunological applications relies heavily on radioactive isotopes owing to their high detection sensitivity. However, due to the relatively long experimental time, short shelf lives of expensive reagents, and the increasing concern on the health hazards of radioactive materials, both organic fluorophores and luminescent lanthanide chelates have been developed as alternatives.[2] Many fluorescent organic compounds have been designed, and a wide range of these biological labeling reagents is already commercially available. Labeling of oligonucleotides, amino acids, peptides, proteins, antibodies, and biological tissues with these fluorophores is well documented. However, many organic dyes have limitations due to their high photobleaching rates, strong pH dependence, short fluorescence lifetimes, and small Stokes shifts. On the other hand, various lanthanide chelates have also been developed as very useful biological labeling reagents owing to their intense and extraordinarily long-lived luminescence, which enables time-resolved detection.[2] However, the development of new lanthanide chelates represents a challenge owing to the requirement of a suitable chelate which not only protects the luminescent lanthanide center from quenching by water molecules, but also acts as an energy sensitizer to enable energy transfer to the lanthanide center.[2]

* To whom all correspondence should be addressed. E-mail: bhkenlo@cityu.edu.hk. Fax: (852) 2788 7406.
† City University of Hong Kong.
‡ The University of Hong Kong.

(1) See, for example: (a) Hermanson, G. T. *Bioconjugate Techniques*; Academic Press: San Diego, CA, 1996. (b) Kessler, C. *Nonradioactive Labeling and Detection of Biomolecules*, 2nd ed.; Springer: Heidelberg, Germany, 1999.

(2) See, for example: Sammes, P. G.; Yahioglu, G. *Nat. Prod. Rep.* **1996**, *13*, 1.

10.1021/ic0346984 CCC: $25.00
Published on Web 09/17/2003

Owing to the variable oxidation states, flexible coordinating geometry, and rich photophysical and electrochemical properties, many transition metal complexes have been attached to various biomolecules for various studies.[3] The studies include photoinduced electron transfer in metalloproteins;[3a] recognition, photocleavage, and cross-linking of nucleic acids;[3b,c] automated synthesis of metal-containing oligonucleotides;[3d] investigations of protein hydrodynamics using anisotropy probes;[3e] development of artificial nucleases;[3f] and folding kinetics and thermodynamics of proteins.[3g] While much work has been focused on ruthenium(II), osmium(II), rhodium(III), and rhenium(I) complexes, related studies on biological labeling using luminescent iridium(III) polypyridine complexes remain relatively unexplored.

On the other hand, the iridium(III) metal center can be coordinated with various cyclometalating and polypyridine ligands to give a wide range of complexes with very interesting physical and chemical properties.[4−15] Some of these complexes have been utilized as a sensor for various analytes, including oxygen,[5d] proton,[11a] and chloride ion.[11b] Recently, the use of luminescent iridium(III) complexes in the development of light-emitting diodes has also received much attention.[10,16]

Recently, we have reported the use of iridium(III) polypyridine complexes as luminescent biological labeling reagents.[15] We anticipate that by a systematic variation on the identity of the ligands, as well as the reactive functional groups, not only a series of new luminescent iridium(III) complexes with rich photophysical and photochemical properties could be produced, but also a new class of biological labeling reagents could be developed. In this paper, we report the synthesis and characterization of a family of new cyclometalated iridium(III) diimine complexes $[Ir(N\text{-}C)_2(N\text{-}N)](PF_6)$ (HN-C = 2-phenylpyridine, Hppy; 2-(4-methylphenyl)pyridine, Hmppy; 3-methyl-1-phenylpyrazole, Hmppz; 7,8-benzoquinoline, Hbzq; 2-phenylquinoline, Hpq; N-N = 4-amino-2,2′-bipyridine, bpy-NH_2; 4-isothiocyanato-2,2′-bipyridine, bpy-ITC; 4-iodoacetamido-2,2′-bipyridine, bpy-IAA; 5-amino-1,10-phenanthroline, phen-NH_2; 5-isothiocyanato-1,10-phenanthroline, phen-ITC; 5-iodoacetamido-1,-10-phenanthroline, phen-IAA) (Chart 1). The structure of one of the complexes, $[Ir(mppz)_2(bpy\text{-}NH_2)](PF_6)$, is studied by X-ray crystallography. The photophysical and electrochemical properties of all the new cyclometalated iridium(III) diimine complexes are also investigated. On the basis of the photophysical and electrochemical data, the excited-state character of these complexes is identified. The cyclometalating ligands play an important role in this study because they can perturb the iridium(III) centers, leading to substantial variation on the excited-state properties of the complexes. For successful applications as luminescent biological labels in bioassays, the complexes should exhibit intense and long-lived luminescence, preferably in the visible region, and such candidates are identified in this work. Accordingly,

(3) See, for example: (a) Gray, H. B.; Winkler, J. R. *Annu. Rev. Biochem.* **1996**, *65*, 537. (b) Erkkila, K. E.; Odom, D. T.; Barton, J. K. *Chem. Rev.* **1999**, *99*, 2777. (c) Cohen, S. M.; Lippard, S. J. *Prog. Nucleic Acid Res.* **2001**, *67*, 93. (d) Beilstein, A. E.; Tierney, M. T.; Grinstaff, M. W. *Comments Inorg. Chem.* **2000**, *22*, 105. (e) Terpetschnig, E.; Szmacinski, H.; Lakowicz, J. R. *Methods Enzymol.* **1997**, *278*, 295. (f) Perrin, D. M.; Mazumder, A.; Sigman, D. S. *Prog. Nucleic Acid Res.* **1996**, *52*, 123. (g) Winkler, J. R.; Gray, H. B. *Chem. Rev.* **1992**, *92*, 369.

(4) (a) Watts, R. J. *Inorg. Chem.* **1981**, *20*, 2302. (b) Sprouse, S.; King, K. A.; Spellane, P. J.; Watts, R. J. *J. Am. Chem. Soc.* **1984**, *106*, 6647. (c) Ohsawa, Y.; Sprouse, S.; King, K. A.; DeArmond, M. K.; Hanck, K. W.; Watts, R. J. *J. Phys. Chem.* **1987**, *91*, 1047. (d) Garces, F. O.; King, K. A.; Watts, R. J. *Inorg. Chem.* **1988**, *27*, 3464. (e) Wilde, A. P.; Watts, R. J. *J. Phys. Chem.* **1991**, *95*, 622. (f) Wilde, A. P.; King, K. A.; Watts, R. J. *J. Phys. Chem.* **1991**, *95*, 629. (g) Dedeian, K.; Djurovich, P. I.; Garces, F. O.; Carlson, G.; Watts, R. J. *Inorg. Chem.* **1991**, *30*, 1685. (h) Djurovich, P. I.; Watts, R. J. *Inorg. Chem.* **1993**, *32*, 4681. (i) Schmid, B.; Garces, F. O.; Watts, R. J. *Inorg. Chem.* **1994**, *33*, 9.

(5) (a) Serroni, S.; Juris, A.; Campagna, S.; Venturi, M.; Denti, G.; Balzani, V. *J. Am. Chem. Soc.* **1994**, *116*, 9086. (b) Calogero, G.; Giuffrida, G.; Serroni, S.; Ricevuto, V.; Campagna, S. *Inorg. Chem.* **1995**, *34*, 541. (c) Mamo, A.; Stefio, I.; Parisi, M. F.; Credi, A.; Venturi, M.; Di Pietro, C.; Campagna, S. *Inorg. Chem.* **1997**, *36*, 5947. (d) Di Marco, G.; Lanza, M.; Mamo, A.; Stefio, I.; Di Pietro, C.; Romeo, G.; Campagna, S. *Anal. Chem.* **1998**, *70*, 5019. (e) Neve, F.; Crispini, A.; Campagna, S.; Serroni, S. *Inorg. Chem.* **1999**, *38*, 2250. (f) Griffiths, P. M.; Loiseau, F.; Puntoriero, F.; Serroni, S.; Campagna, S. *Chem. Commun.* **2000**, 2297. (g) Neve, F.; Crispini, A.; Loiseau, F.; Campagna, S. *J. Chem. Soc., Dalton Trans.* **2000**, 1399. (h) Neve, F.; Crispini, A. *Eur. J. Inorg. Chem.* **2000**, 1039. (i) Neve, F.; Crispini, A.; Serroni, S.; Loiseau, F.; Campagna, S. *Inorg. Chem.* **2001**, *40*, 1093.

(6) (a) Vogler, L. M.; Scott, B.; Brewer, K. J. *Inorg. Chem.* **1993**, *32*, 898. (b) Bridgewater, J. S.; Vogler, L. M.; Molnar, S. M.; Brewer, K. J. *Inorg. Chim. Acta* **1993**, *208*, 179. (c) Molnar, S. M.; Nallas, G.; Bridgewater, J. S.; Brewer, K. J. *J. Am. Chem. Soc.* **1994**, *116*, 5206.

(7) (a) Didier, P.; Ortmans, I.; Kirsch-De Mesmaeker, A.; Watts, R. J. *Inorg. Chem.* **1993**, *32*, 5239. (b) Ortmans, I.; Didier, P.; Kirsch-De Mesmaeker, A. *Inorg. Chem.* **1995**, *34*, 3695.

(8) (a) Collin, J.-P.; Dixon, I. M.; Sauvage, J.-P.; Williams, J. A. G.; Barigelletti, F.; Flamigni, L. *J. Am. Chem. Soc.* **1999**, *121*, 5009. (b) Dixon, I. M.; Collin, J.-P.; Sauvage, J.-P.; Flamigni, L.; Encinas, S.; Barigelletti, F. *Chem. Soc. Rev.* **2000**, *29*, 385. (c) Dixon, I. M.; Collin, J.-P.; Sauvage, J.-P.; Barigelletti, F.; Flamigni, L. *Angew. Chem., Int. Ed.* **2000**, *39*, 1292. (d) Flamigni, L.; Dixon, I. M.; Collin, J.-P.; Sauvage, J.-P. *Chem. Commun.* **2000**, 2479. (e) Dixon, I. M.; Collin, J.-P.; Sauvage, J.-P.; Flamigni, L. *Inorg. Chem.* **2001**, *40*, 5507.

(9) (a) Colombo, M. G.; Güdel, H. U. *Inorg. Chem.* **1993**, *32*, 3081. (b) Colombo, M. G.; Hauser, A.; Güdel, H. U. *Inorg. Chem.* **1993**, *32*, 3088. (c) Colombo, M. G.; Brunold, T. C.; Riedener, T.; Güdel, H. U.; Förtsch, M.; Bürgi, H.-B. *Inorg. Chem.* **1994**, *33*, 545. (d) Colombo, M. G.; Hauser, A.; Güdel, H. U. *Topics Curr. Chem.* **1994**, *171*, 143.

(10) (a) Lamansky, S.; Djurovich, P.; Murphy, D.; Abdel-Razzaq, F.; Kwong, R.; Tsyba, I.; Bortz, M.; Mui, B.; Bau, R.; Thompson, M. E. *Inorg. Chem.* **2001**, *40*, 1704. (b) Lamansky, S.; Djurovich, P.; Murphy, D.; Abdel-Razzaq, F.; Lee, H.-E.; Adachi, C.; Burrows, P. E.; Forrest, S. R.; Thompson, M. E. *J. Am. Chem. Soc.* **2001**, *123*, 4304. (c) Gao, R.; Ho, D. G.; Hernandez, B.; Selke, M.; Murphy, D.; Djurovich, P. I.; Thompson, M. E. *J. Am. Chem. Soc.* **2002**, *124*, 14828.

(11) (a) Licini, M.; Williams, J. A. G. *Chem. Commun.* **1999**, 1943. (b) Goodall, W.; Williams, J. A. G. *J. Chem. Soc., Dalton Trans.* **2000**, 2893.

(12) Ayala, N. P.; Flynn, C. M., Jr.; Sacksteder, L.; Demas, J. N.; DeGraff, B. A. *J. Am. Chem. Soc.* **1990**, *112*, 3837.

(13) (a) van Diemen, J. H.; Haasnoot, J. G.; Hage, R.; Müller, E.; Reedijk, J. *Inorg. Chim. Acta* **1991**, *181*, 245. (b) van Diemen, J. H.; Hage, R.; Haasnoot, J. G.; Lempers, H. E. B.; Reedijk, J.; Vos, J. G.; De Cola, L.; Barigelletti, F.; Balzani, V. *Inorg. Chem.* **1992**, *31*, 3518.

(14) Maestri, M.; Balzani, V.; Deuschel-Cornioley, C.; von Zelewsky, A. *Adv. Photochem.* **1992**, *17*, 1.

(15) (a) Lo, K. K. W.; Ng, D. C. M.; Chung, C. K. *Organometallics* **2001**, *20*, 4999. (b) Lo, K. K. W.; Chung, C. K.; Ng, D. C. M.; Zhu, N. *New J. Chem.* **2002**, *26*, 81. (c) Lo, K. K. W.; Chung, C. K.; Zhu, N. *Chem. Eur. J.* **2003**, *9*, 475.

(16) (a) Baldo, M. A.; Thompson, M. E.; Forrest, S. R. *Nature* **2000**, *403*, 750. (b) Watanabe, T.; Nakamura, K.; Kawami, S.; Fukuda, Y.; Tsuji, T.; Wakimoto, T.; Miyaguchi, S.; Yahiro, M.; Yang, M.-J.; Tsutsui, T. *Synth. Met.* **2001**, *122*, 203. (c) Ostrowski, J. C.; Robinson, M. R.; Heeger, A. J.; Bazan, G. C. *Chem. Commun.* **2002**, 784. (d) Beeby, A.; Bettington, S.; Samuel, I. D. W.; Wang, Z. *J. Mater. Chem.* **2003**, *13*, 80.

Chart 1. Structures of Cyclometalated Iridium(III) Diimine Complexes

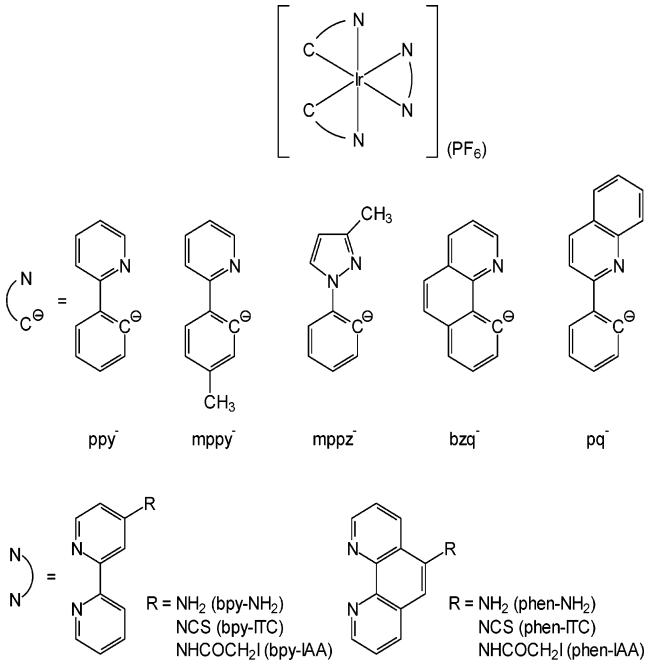

we label various biological molecules with a selection of the iridium(III) isothiocyanate and iodoacetamide complexes to give luminescent bioconjugates, the photophysical properties of which are also investigated. In view of the interesting photophysical properties of these conjugates, we design a competitive heterogeneous assay for digoxin, a potent cardiac glycoside that is commonly prescribed for the treatment of patients suffering from congestive heart failure.[17] In the assay, the digoxin analyte competes with a digoxin derivative immobilized on the solid phase for binding to a biotinylated anti-digoxin. The assay uses avidin labeled with one of the luminescent iridium(III) complexes to recognize the immobilized biotinylated anti-digoxin. The conditions and performance of this new bioassay are investigated.

Results and Discussion

Synthesis. The amine complexes $[Ir(N\text{-}C)_2(bpy\text{-}NH_2)](PF_6)$ and $[Ir(N\text{-}C)_2(phen\text{-}NH_2)](PF_6)$ are synthesized from the reaction of $[Ir_2(N\text{-}C)_4Cl_2]$ with 2 equiv of the corresponding amine-containing diimines in refluxing CH_2Cl_2/MeOH, followed by metathesis with KPF_6, and chromatographic purification.[15a] All the isothiocyanate complexes are obtained from the reaction of the amine complexes with thiophosgene in acetone at room temperature.[15a] The iodoacetamide complexes are, however, prepared from two different approaches. Whereas the complexes $[Ir(N\text{-}C)_2(phen\text{-}IAA)](PF_6)$ can be obtained from the reaction of $[Ir(N\text{-}C)_2(phen\text{-}NH_2)](PF_6)$ with iodoacetic anhydride in CH_3CN,[15a] a similar treatment of $[Ir(N\text{-}C)_2(bpy\text{-}NH_2)](PF_6)$ does not give the desired iodoacetamide complexes, probably due to the reduced nucleophilicity of the amine group at the C4-position of the coordinated bipyridine ligand. Nevertheless, we find that the complexes $[Ir(N\text{-}C)_2(bpy\text{-}IAA)](PF_6)$ can be synthesized readily from the reaction of their precursor amine complexes with iodoacetyl chloride in CH_2Cl_2.[18] All the iridium(III) complexes in this work are air-stable, and our characterization data show that the isothiocyanate and iodoacetamide complexes are stable for a period of months when stored at −20 °C in the absence of moisture. All the complexes are soluble in common organic solvents such as alcohols, acetone, and chlorinated solvents, but sparingly soluble in water.

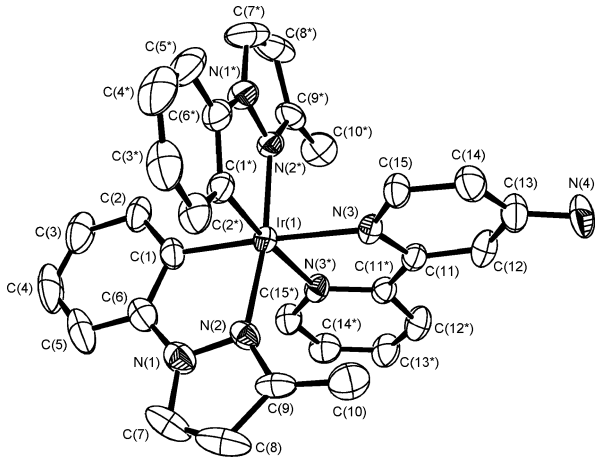

Figure 1. Perspective view of $[Ir(mppz)_2(bpy\text{-}NH_2)]^+$ (20% thermal ellipsoids).

Table 1. Selected Bond Lengths (Å) and Bond Angles (deg) for $[Ir(mppz)_2(bpy\text{-}NH_2)](PF_6)$

Ir(1)−N(2)	2.047(7)	Ir(1)−N(3)	2.131(6)
Ir(1)−C(1)	2.022(8)	Ir(1)−N(2*)	2.047(7)
Ir(1)−N(3*)	2.131(6)	Ir(1)−C(1*)	2.022(8)
N(2)−Ir(1)−N(3)	98.9(3)	N(2)−Ir(1)−N(2*)	171.7(4)
N(2)−Ir(1)−N(3*)	87.6(2)	N(2)−Ir(1)−C(1)	81.1(4)
N(2)−Ir(1)−C(1*)	92.9(3)	N(3)−Ir(1)−C(1)	174.3(3)
N(3)−Ir(1)−N(2*)	87.6(2)	N(3)−Ir(1)−N(3*)	76.7(4)
N(3)−Ir(1)−C(1*)	97.6(3)	C(1)−Ir(1)−N(2*)	92.9(3)
C(1)−Ir(1)−N(3*)	97.6(3)	C(1)−Ir(1)−C(1*)	88.1(5)
N(2*)−Ir(1)−N(3*)	98.9(3)	N(2*)−Ir(1)−C(1*)	81.1(4)
N(3*)−Ir(1)−C(1*)	174.3(3)		

The complexes are characterized by ^1H NMR spectroscopy, positive-ion ESI-MS, and IR spectroscopy, and they give satisfactory elemental analysis. The IR spectra of the isothiocyanate complexes display absorption bands at ca. 2073−1990 cm^{-1}, and the iodoacetamide complexes at ca. 1701−1604 and 1583−1515 cm^{-1}, typical of ν_{NCS}, ν_{CO}, and ν_{NH} stretching, respectively. The X-ray crystal structure of $[Ir(mppz)_2(bpy\text{-}NH_2)](PF_6)$ is also investigated.

Crystal Structure Determination. The perspective view of the complex cation of $[Ir(mppz)_2(bpy\text{-}NH_2)](PF_6)$ is depicted in Figure 1. Selected bond lengths and angles are listed in Table 1. The iridium(III) center adopts a distorted octahedral geometry, and the angles of the *trans* ligands at the metal center range between 171.7(4) and 174.3(3) Å. The coordination geometry of the $mppz^-$ ligands around the iridium(III) center is such that the metal−carbon bonds are in a *cis* orientation.[5e,h,13a,15c] The *trans* influence of the carbon

(17) See for example: (a) Riaz, K.; Forker, A. D. *Drugs* **1998**, *55*, 747. (b) Dasgupta, A. *Am. J. Clin. Pathol.* **2002**, *118*, 132. (c) Kjeldsen, K.; Norgaard, A.; Gheorghiade, M. *Cardiovasc. Res.* **2002**, *55*, 710.

(18) Fava, C.; Galeazzi, R.; Mobbili, G.; Orena, M. *Tetrahedron: Asymmetry* **2001**, *12*, 2731.

donors renders slightly longer Ir−N bond lengths in the bpy-NH_2 ligand (Ir−N(3) and Ir−N(3*) 2.131(6) Å) than in the $mppz^-$ ligand (Ir−N(2) and Ir−N(2*) 2.047(7) Å). The bite angle of the $mppz^-$ ligand (81.1(4)°) is larger than that of the bpy-NH_2 ligand (76.7(4)°). These observations have been made in related cyclometalated iridium(III) polypyridine systems $[Ir(N\text{-}C)_2(N\text{-}N)]^+$.[5e,h,13a,15c]

Electronic Absorption Spectroscopy. The electronic absorption spectral data of all the complexes in CH_2Cl_2 and CH_3CN are included in the Supporting Information. In general, all the spectra are characterized by intense intraligand (IL) ($\pi \rightarrow \pi^*$)(N-N and N-C^-) absorption bands at ca. 225−302 nm (ϵ on the order of 10^4 dm^3 mol^{-1} cm^{-1}) and less intense spin-allowed metal-to-ligand charge-transfer (^{1}MLCT) ($d\pi$(Ir) $\rightarrow$ π^*(N-N and N-C^-)) absorption shoulders at ca. 308−528 nm. Due to spin−orbit coupling associated with the iridium center, spin-forbidden ^{3}MLCT ($d\pi$(Ir) $\rightarrow$ π^*(N-N and N-C^-)) absorption tailing is also observed at a lower energy region (ca. 528−550 nm). These absorption features are similar to those of related iridium(III) polypyridine systems.[4c−e,5,7,9d,13a,14,15a,c]

Luminescence Properties. Upon irradiation, all the complexes display intense and long-lived orange-red to greenish-yellow luminescence under ambient conditions and in alcohol glass at 77 K. The photophysical data are listed in Table 2. In solutions at room temperature, most of the complexes show solvatochromism, with the emission maxima occurring at higher energy in less polar CH_2Cl_2 than in more polar CH_3CN. The emission lifetimes are in the submicrosecond to microsecond time scale, indicative of the phosphorescence nature of the emission. With reference to previous spectroscopic studies on the luminescent $[Ir(N\text{-}C)_2(N\text{-}N)]^+$ systems,[4c−f,5b,e,g,i,7a,8b,9a,b,d,13a,15a] the emission of these complexes is generally assigned to a triplet MLCT ($d\pi$(Ir) $\rightarrow$ π^*(N-N)) excited state. The assignment of an ^{3}MLCT state associated with the diimine ligand is supported by the findings that all the amine-containing complexes emit at the highest energy, followed by their iodoacetamide counterparts, while the isothiocyanate complexes emit at the lowest energy. This is in line with the electron-donating properties of the primary amine group and the electron-withdrawing properties of the iodoacetamide and isothiocyanate groups. The emission spectra of $[Ir(mppz)_2(bpy\text{-}NH_2)](PF_6)$, $[Ir(mppz)_2(bpy\text{-}IAA)](PF_6)$, and $[Ir(mppz)_2(bpy\text{-}ITC)](PF_6)$ in CH_2Cl_2 are shown in Figure 2 as an example.

It is noteworthy that two groups of this family of complexes show special emissive properties. First, the complexes $[Ir(N\text{-}C)_2(phen\text{-}NH_2)](PF_6)$ exhibit extraordinarily long emission lifetimes (from ca. 3.3 to 25.0 μs) in fluid solutions at 298 K, leading to radiative decay rate constants that are 1−2 orders of magnitude smaller than those of the other complexes in this work (Table 2). Also, unlike common iridium(III) diimine MLCT emitters,[4c,d,f,5b,e,g,i,7a,8b,13a,14,15a] the emission maxima of these phen-NH_2 complexes show exceptionally small blue-shifts upon cooling to 77 K (see following description). Interestingly, this behavior is not observed for their close structural counterparts $[Ir(N\text{-}C)_2(bpy\text{-}NH_2)](PF_6)$ (Table 2). On the basis of these observations, we believe that the long-lived emission of the phen-NH_2 complexes at room temperature originates from an excited state of substantial ^{3}IL ($\pi \rightarrow \pi^*$)(phen-NH_2) character.[8a,b,11,12,15a]

On the other hand, we note that complexes with the cyclometalating ligand pq^- exhibit quite different photophysical properties compared to those of other complexes. In solutions at room temperature, the complexes $[Ir(pq)_2(N\text{-}N)](PF_6)$ all show similar structural features in their emission spectra, with an emission maximum at ca. 555−563 nm and a shoulder at ca. 599−604 nm (Table 2). The emission spectra of $[Ir(pq)_2(bpy\text{-}NH_2)](PF_6)$ in CH_2Cl_2 at 298 K and in low temperature alcohol glass are shown in Figure 3. The emission lifetimes of these pq^- complexes vary from ca. 0.9 to 2.6 μs and are apparently longer than those of complexes with other cyclometalating ligands (except for the case of $[Ir(pq)_2(phen\text{-}NH_2)](PF_6)$, see preceding discussion). Since the diimine ligands do not play an important role in the photophysical properties of these complexes, and structured emission bands are observed in the room temperature solution spectra, the excited state of these complexes is likely to possess ^{3}IL ($\pi \rightarrow \pi^*$)(pq^-) character and perhaps some ^{3}MLCT ($d\pi$(Ir) $\rightarrow$ π^*(pq^-)) character as well. The involvement of pq^- in the excited state is justified by a high degree of π-conjugation in this cyclometalating ligand. It is interesting to note that similar intraligand emission has been observed for related iridium(III) complexes such as $[Ir(pq)_2(acac)]$ (Hacac = acetylacetone).[10]

The emission spectra of all the complexes in alcohol glass at 77 K display structural features. The two groups of complexes $[Ir(N\text{-}C)_2(phen\text{-}NH_2)](PF_6)$ and $[Ir(pq)_2(N\text{-}N)](PF_6)$ already mentioned also show photophysical properties that are remarkably different from those of other complexes. For example, all the $[Ir(N\text{-}C)_2(phen\text{-}NH_2)](PF_6)$ complexes exhibit extremely long emission lifetimes (ca. 260−389 μs) in low temperature glass. The emission maxima do not show large blue-shifts compared to those of the solution spectra at room temperature. These findings suggest that the ^{3}IL ($\pi \rightarrow \pi^*$)(phen-NH_2) character is more evident in the excited states of these complexes at low temperature. Meanwhile, the complexes $[Ir(pq)_2(N\text{-}N)](PF_6)$ all display very similar and vibronically structured emission spectra with an emission lifetime of ca. 5 μs at 77 K, irrespective of the identity of the diimine ligand (except for phen-NH_2). Upon cooling to 77 K, these pq^- complexes exhibit blue-shifts in their emission maxima. It is conceivable that the emissive states of $[Ir(pq)_2(N\text{-}N)](PF_6)$ at 77 K involve mixed ^{3}IL and ^{3}MLCT character associated with the pq^- ligand.

Biexponential emission decays are commonly noticed in cyclometalated iridium(III) diimine systems in low temperature glass, and the emission has been identified to originate from two ^{3}MLCT excited states involving the cyclometalating and diimine ligands, respectively.[4c−f,5b,9d,13a,14,15a] Many complexes in the current work also display dual luminescence properties at 77 K. For example, except for N−C^- = pq^-, the complexes $[Ir(N\text{-}C)_2(phen\text{-}ITC)](PF_6)$ display biexponential decays with lifetimes of ca. 4.2−15 and 33−94 μs, and $[Ir(N\text{-}C)_2(phen\text{-}IAA)](PF_6)$ also show dual luminescence with lifetimes of ca. 3.7−5.0 and 11−23 μs (Table 2). With

Table 2. Photophysical Data of $[Ir(N\text{-}C)_2(N\text{-}N)](PF_6)$

complex	medium (T/K)	λ_{em}/nm	τ_o/μs	Φ_{em}	k_r/s^{-1}	k_{nr}/s^{-1}
$[Ir(ppy)_2(bpy\text{-}NH_2)](PF_6)$	CH_2Cl_2 (298)	553	0.98	0.263	2.7×10^5	7.5×10^5
	CH_3CN (298)	555	0.77	0.236	3.1×10^5	9.9×10^5
	glass (77)[a]	474, 489, 510, 525 sh, 564 sh	6.73			
$[Ir(ppy)_2(bpy\text{-}ITC)](PF_6)$	CH_2Cl_2 (298)	595	0.45	0.086	1.9×10^5	2.0×10^5
	CH_3CN (298)	593	0.31	0.035	1.1×10^5	3.1×10^6
	glass (77)[a]	500, 538, 587 sh	31.84 (21%), 3.72 (79%)			
$[Ir(ppy)_2(bpy\text{-}IAA)](PF_6)$	CH_2Cl_2 (298)	572	0.34	0.048	1.4×10^5	2.8×10^6
	CH_3CN (298)	582	0.30	0.022	7.3×10^4	3.3×10^6
	glass (77)[a]	474 sh, 512, 540 sh, 605 sh	4.96			
$[Ir(mppy)_2(bpy\text{-}NH_2)](PF_6)$	CH_2Cl_2 (298)	562	0.82	0.251	3.1×10^5	9.1×10^5
	CH_3CN (298)	561	0.67	0.183	2.7×10^5	1.2×10^6
	glass (77)[a]	475, 492, 511 sh, 528 sh, 569 sh	7.30			
$[Ir(mppy)_2(bpy\text{-}ITC)](PF_6)$	CH_2Cl_2 (298)	606	0.25	0.060	2.4×10^5	3.8×10^6
	CH_3CN (298)	609	0.20	0.023	1.2×10^5	4.9×10^6
	glass (77)[a]	476 sh, 521, 551 sh	4.95			
$[Ir(mppy)_2(bpy\text{-}IAA)](PF_6)$	CH_2Cl_2 (298)	579	0.37	0.050	1.5×10^5	2.8×10^6
	CH_3CN (298)	588	0.21	0.022	1.0×10^5	4.7×10^6
	glass (77)[a]	476 sh, 514, 612 sh	4.86			
$[Ir(mppz)_2(bpy\text{-}NH_2)](PF_6)$	CH_2Cl_2 (298)	546	1.05	0.285	2.7×10^5	6.8×10^5
	CH_3CN (298)	555	0.72	0.236	3.3×10^5	1.1×10^6
	glass (77)[a]	486, 518, 562 sh	9.50			
$[Ir(mppz)_2(bpy\text{-}ITC)](PF_6)$	CH_2Cl_2 (298)	599	0.30	0.079	2.6×10^5	3.1×10^6
	CH_3CN (298)	595	0.26	0.033	1.3×10^5	3.7×106
	glass (77)[a]	503 sh, 534	4.16			
$[Ir(mppz)_2(bpy\text{-}IAA)](PF_6)$	CH_2Cl_2 (298)	567	0.29	0.059	2.0×10^5	3.2×10^6
	CH_3CN (298)	575	0.21	0.024	1.1×10^5	4.6×10^6
	glass (77)[a]	480 sh, 511, 537 sh, 609 sh	4.70			
$[Ir(bzq)_2(bpy\text{-}NH_2)](PF_6)$	CH_2Cl_2 (298)	556	1.42	0.221	1.6×10^5	5.5×10^5
	CH_3CN (298)	551	2.40	0.158	6.6×10^4	3.5×10^5
	glass (77)[a]	499, 540, 581 sh	46.21			
$[Ir(bzq)_2(bpy\text{-}ITC)](PF_6)$	CH_2Cl_2 (298)	594	0.41	0.107	2.6×10^5	2.2×10^6
	CH_3CN (298)	596	0.26	0.049	1.9×10^5	3.7×10^6
	glass (77)[a]	475 sh, 511, 546 sh	4.93			
$[Ir(bzq)_2(bpy\text{-}IAA)](PF_6)$	CH_2Cl_2 (298)	570	0.47	0.064	1.4×10^5	2.0×10^6
	CH_3CN (298)	579	0.30	0.024	8.0×10^4	3.3×10^6
	glass (77)[a]	501, 538, 582 sh	41.07 (32%), 4.51 (68%)			
$[Ir(pq)_2(bpy\text{-}NH_2)](PF_6)$	CH_2Cl_2 (298)	556, 602 sh	2.60	0.361	1.4×10^5	2.5×10^5
	CH_3CN (298)	562, 602 sh	2.58	0.270	1.0×10^5	2.8×10^5
	glass (77)[a]	546, 589, 639 sh	4.90			
$[Ir(pq)_2(bpy\text{-}ITC)](PF_6)$	CH_2Cl_2 (298)	556, 602 sh	2.02	0.240	1.2×10^5	3.8×10^5
	CH_3CN (298)	563, 604 sh	2.09	0.179	8.6×10^4	3.9×10^5
	glass (77)[a]	542, 581, 637 sh	4.82			
$[Ir(pq)_2(bpy\text{-}IAA)](PF_6)$	CH_2Cl_2 (298)	555, 596 sh	0.93	0.237	2.5×10^5	8.2×10^5
	CH_3CN (298)	559, 599 sh	1.02	0.147	1.4×10^5	8.4×10^5
	glass (77)[a]	541, 585, 640 sh	4.84			
$[Ir(ppy)_2(phen\text{-}NH_2)](PF_6)$	CH_2Cl_2 (298)	564	9.52	0.428	4.5×10^4	6.0×10^4
	CH_3CN (298)	568	11.38	0.079	6.9×10^3	8.1×10^4
	glass (77)[a]	560, 602, 658 sh	286.21			
$[Ir(ppy)_2(phen\text{-}ITC)](PF_6)$	CH_2Cl_2 (298)	598	0.77	0.287	3.7×10^5	9.3×10^5
	CH_3CN (298)	608	0.41	0.079	1.9×10^5	2.2×10^6
	glass (77)[a]	512, 552, 594 sh	93.52 (32%), 14.58 (68%)			
$[Ir(ppy)_2(phen\text{-}IAA)](PF_6)$	CH_2Cl_2 (298)	584	0.86	0.197	2.3×10^5	9.3×10^5
	CH_3CN (298)	590	0.59	0.228	3.9×10^5	1.3×10^6
	glass (77)[a]	500, 536, 580 sh	22.10 (23%), 4.99 (77%)			
$[Ir(mppy)_2(phen\text{-}NH_2)](PF_6)$	CH_2Cl_2 (298)	575	3.25	0.222	6.8×10^4	2.4×10^5
	CH_3CN (298)	576	5.32	0.027	5.1×10^3	1.8×10^5
	glass (77)[a]	561, 605, 662 sh	265.00			
$[Ir(mppy)_2(phen\text{-}ITC)](PF_6)$	CH_2Cl_2 (298)	604	0.55	0.077	1.4×10^5	1.7×10^6
	CH_3CN (298)	614	0.28	0.035	1.3×10^5	3.4×10^6
	glass (77)[a]	514, 553, 600 sh	32.73 (17%), 4.16 (83%)			

Table 2. (Continued)

complex	medium (T/K)	λ_{em}/nm	τ_o/μs	Φ_{em}	k_r/s^{-1}	k_{nr}/s^{-1}
$[Ir(mppy)_2(phen\text{-}IAA)](PF_6)$	CH_2Cl_2 (298)	596	0.69	0.155	2.5×10^5	1.3×10^6
	CH_3CN (298)	600	0.42	0.088	2.1×10^5	2.2×10^6
	glass (77)[a]	501 sh, 517 sh, 535, 559 sh	11.02 (42%), 3.68 (58%)			
$[Ir(mppz)_2(phen\text{-}NH_2)](PF_6)$	CH_2Cl_2 (298)	554	10.36	0.253	2.4×10^4	7.2×10^4
	CH_3CN (298)	564	10.34	0.016	1.5×10^3	9.5×10^4
	glass (77)[a]	560, 606, 658 sh	308.83			
$[Ir(mppz)_2(phen\text{-}ITC)](PF_6)$	CH_2Cl_2 (298)	587	0.63	0.153	2.4×10^5	1.3×10^6
	CH_3CN (298)	602	0.28	0.132	4.7×10^5	3.1×10^5
	glass (77)[a]	512, 552, 598	44.82 (19%), 4.28 (81%)			
$[Ir(mppz)_2(phen\text{-}IAA)](PF_6)$	CH_2Cl_2 (298)	576	0.66	0.153	2.3×10^5	1.3×10^6
	CH_3CN (298)	586	0.39	0.078	2.0×10^5	2.4×10^5
	glass (77)[a]	501, 514, 535, 580 sh	15.57 (28%), 4.19 (72%)			
$[Ir(bzq)_2(phen\text{-}NH_2)](PF_6)$	CH_2Cl_2 (298)	568	6.65	0.263	4.0×10^4	1.1×10^5
	CH_3CN (298)	567	25.02	0.015	6.0×10^2	3.9×10^4
	glass (77)[a]	506 sh, 562, 606, 666 sh	260.30			
$[Ir(bzq)_2(phen\text{-}ITC)](PF_6)$	CH_2Cl_2 (298)	597	0.67	0.118	1.8×10^5	1.3×10^6
	CH_3CN (298)	607	0.32	0.046	1.4×10^5	3.0×10^6
	glass (77)[a]	511, 553, 600 sh	51.83 (23%), 4.48 (77%)			
$[Ir(bzq)_2(phen\text{-}IAA)](PF_6)$	CH_2Cl_2 (298)	588	0.50	0.112	2.2×10^5	1.8×10^6
	CH_3CN (298)	592	0.41	0.080	2.0×10^5	2.2×10^6
	glass (77)[a]	501, 537, 579 sh	22.64 (33%), 3.81 (67%)			
$[Ir(pq)_2(phen\text{-}NH_2)](PF_6)$	CH_2Cl_2 (298)	555, 599 sh	4.07	0.359	8.8×10^4	1.6×10^5
	CH_3CN (298)	559, 599 sh	5.99	0.169	2.8×10^4	1.4×10^5
	glass (77)[a]	540 sh, 570, 615 sh, 681 sh	389.15			
$[Ir(pq)_2(phen\text{-}ITC)](PF_6)$	CH_2Cl_2 (298)	560, 599 sh	1.50	0.248	1.7×10^5	5.0×10^5
	CH_3CN (298)	559, 599 sh	1.13	0.172	1.5×10^5	7.3×10^5
	glass (77)[a]	540, 582, 626 sh	4.96			
$[Ir(pq)_2(phen\text{-}IAA)](PF_6)$	CH_2Cl_2 (298)	555, 599 sh	1.90	0.271	1.4×10^5	3.8×10^5
	CH_3CN (298)	558, 600 sh	2.22	0.281	1.3×10^5	3.2×10^5
	glass (77)[a]	539, 583, 630 sh	4.95			

[a] EtOH/MeOH (4:1, v/v).

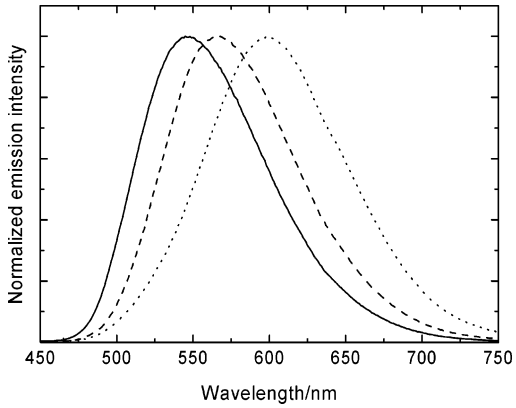

Figure 2. Emission spectra of $[Ir(mppz)_2(bpy\text{-}NH_2)](PF_6)$ (—), $[Ir(mppz)_2(bpy\text{-}IAA)](PF_6)$ (- - -), and $[Ir(mppz)_2(bpy\text{-}ITC)](PF_6)$ (···) in CH_2Cl_2 at 298 K.

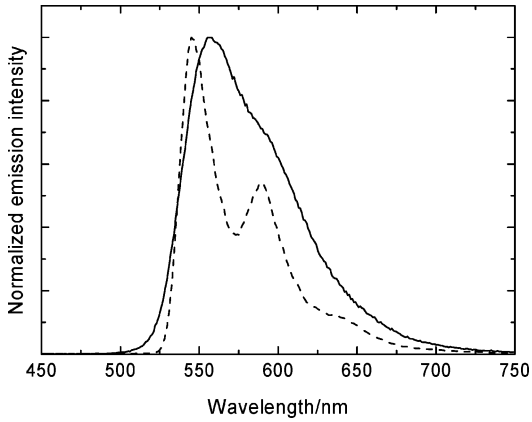

Figure 3. Emission spectra of $[Ir(pq)_2(bpy\text{-}NH_2)](PF_6)$ in CH_2Cl_2 at 298 K (—) and in EtOH/MeOH (4:1, v/v) at 77 K (- - -).

reference to previousphotophysical studies of related cyclometalated iridium(III) diimine complexes at low temperature,[4c−f,5b,e,i,7,8b,13a,14,15a] we assign the shorter-lived component to an ^{3}MLCT state associated with the diimine ligands, while the longer-lived one is assigned to another ^{3}MLCT state associated with the cyclometalating ligands. It is interesting to note that most of the complexes with the bipyridine derivatives (bpy-R, R = NH_2, ITC, or IAA) show a monoexponential decay with a lifetime shorter than 10 μs (Table 2). The lowest-lying emissive states of these complexes appear to possess predominant ^{3}MLCT ($d\pi(Ir) \rightarrow \pi^*$(bpy-R)) (R = NH_2, ITC, or IAA) character. The complex $[Ir(ppy)_2(bpy\text{-}ITC)](PF_6)$, however, is an exception, and it shows dual luminescence with lifetimes of ca. 3.7 and 32 μs, attributable to two ^{3}MLCT excited states associated with the bpy-ITC and ppy^- ligands, respectively. Another interesting observation is that the emission lifetimes of the com-

Table 3. Electrochemical Data of $[Ir(N\text{-}C)_2(N\text{-}N)](PF_6)$ in CH_3CN (0.1 mol dm^{-3} TBAP) at 298 K

complex	oxidation $E_{1/2}$ or E_a/V vs SCE	reduction $E_{1/2}$ or E_c/V vs SCE
$[Ir(ppy)_2(bpy\text{-}NH_2)](PF_6)$	+1.19	−1.59,[a] −2.11,[b] −2.56[b]
$[Ir(ppy)_2(bpy\text{-}ITC)](PF_6)$	+1.19	−1.22,[b] −1.60,[a] −1.97,[a] −2.23[a]
$[Ir(ppy)_2(bpy\text{-}IAA)](PF_6)$	+1.21	−1.12,[b] −1.46,[a] −1.67,[a] −1.94,[a] −2.37[b]
$[Ir(mppy)_2(bpy\text{-}NH_2)](PF_6)$	+1.14	−1.62, −2.22,[b] −2.31[a]
$[Ir(mppy)_2(bpy\text{-}ITC)](PF_6)$	+1.20	−1.21,[b] −1.60,[a] −2.05,[a] −2.26,[a] −2.52[a]
$[Ir(mppy)_2(bpy\text{-}IAA)](PF_6)$	+1.19	−1.10,[b] −1.48,[b] −1.72,[a] −2.11,[b] −2.35[b]
$[Ir(mppz)_2(bpy\text{-}NH_2)](PF_6)$	+1.20	−1.60, −2.13[b]
$[Ir(mppz)_2(bpy\text{-}ITC)](PF_6)$	+1.27	−1.18,[a] −1.66,[a] −2.10[a]
$[Ir(mppz)_2(bpy\text{-}IAA)](PF_6)$	+1.25	−1.07,[b] −1.49,[b] −1.80,[b] −2.17[b]
$[Ir(bzq)_2(bpy\text{-}NH_2)](PF_6)$	+1.09[a]	−1.61, −2.07,[b] −2.45[b]
$[Ir(bzq)_2(bpy\text{-}ITC)](PF_6)$	+1.31	−1.23,[b] −1.69,[b] −2.62[b]
$[Ir(bzq)_2(bpy\text{-}IAA)](PF_6)$	+1.16[a]	−0.91,[b] −1.24,[b] −1.45, −1.84,[b] −2.02,[b] −2.28[b]
$[Ir(pq)_2(bpy\text{-}NH_2)](PF_6)$	+1.20	−1.60,[b] −1.77, −2.24,[b] −2.36[b]
$[Ir(pq)_2(bpy\text{-}ITC)](PF_6)$	+1.28	−1.20,[b] −1.61,[a] −2.33[a]
$[Ir(pq)_2(bpy\text{-}IAA)](PF_6)$	+1.27	−1.06,[b] −1.25,[b] −1.52,[b] −1.78,[b] −1.94,[b] −2.39[b]
$[Ir(ppy)_2(phen\text{-}NH_2)](PF_6)$	+1.27[b]	−1.45,[b] −2.24,[a] −2.53[b]
$[Ir(ppy)_2(phen\text{-}ITC)](PF_6)$	+1.27	−1.21,[b] −1.48, −1.98,[b] −2.43[b]
$[Ir(ppy)_2(phen\text{-}IAA)](PF_6)$	+1.25	−1.08,[b] −1.37,[b] −1.62, −2.46,[b] −2.74[b]
$[Ir(mppy)_2(phen\text{-}NH_2)](PF_6)$	+1.26[b]	−1.43,[a] −2.38[b]
$[Ir(mppy)_2(phen\text{-}ITC)](PF_6)$	+1.19	−1.20,[b] −1.50,[a] −2.42[b]
$[Ir(mppy)_2(phen\text{-}IAA)](PF_6)$	+1.18	−0.98,[b] −1.39,[b] −1.56, −2.35,[b] −2.75[b]
$[Ir(mppz)_2(phen\text{-}NH_2)](PF_6)$	+1.21[b]	−1.49, −2.24,[b] −2.34,[b] −2.67[b]
$[Ir(mppz)_2(phen\text{-}ITC)](PF_6)$	+1.28	−1.21,[b] −1.50,[b] −1.60,[b] −2.58[b]
$[Ir(mppz)_2(phen\text{-}IAA)](PF_6)$	+1.27	−1.02,[b] −1.41,[b] −1.57, −1.99,[b] −2.11,[b] −2.31[a]
$[Ir(bzq)_2(phen\text{-}NH_2)](PF_6)$	+1.13[a]	−1.42,[a] −1.69,[a] −2.00,[b] −2.29[b]
$[Ir(bzq)_2(phen\text{-}ITC)](PF_6)$	+1.15	−1.20,[b] −1.47,[b] −2.08,[b] −2.37[b]
$[Ir(bzq)_2(phen\text{-}IAA)](PF_6)$	+1.13	−1.04,[b] −1.37,[a] −1.60, −1.89,[a] −2.27[a]
$[Ir(pq)_2(phen\text{-}NH_2)](PF_6)$	+1.25[b]	−1.45, −1.75,[a] −1.99,[a] −2.35[a]
$[Ir(pq)_2(phen\text{-}ITC)](PF_6)$	+1.28	−1.20,[b] −1.45,[a] −1.87,[a] −2.56[b]
$[Ir(pq)_2(phen\text{-}IAA)](PF_6)$	+1.29	−0.98,[b] −1.31,[a] −1.55, −1.79,[a] −2.31[b]

[a] Quasireversible wave. [b] Irreversible wave, sweep rate = 100 mV s^{-1}.

plexes $[Ir(bzq)_2(bpy\text{-}R)](PF_6)$ (R = NH_2, IAA, and ITC) change from 46 μs for R = NH_2 to 41 and 4.5 μs (biexponential decay) for R = IAA, and finally to 4.9 μs for R = ITC (Table 2). On the basis of the described assignments, it is likely that the character of the lowest-lying emissive state of this series of complexes changes from ^{3}MLCT (dπ(Ir) → π^*(bzq^-)) to ^{3}MLCT (dπ(Ir) → π^*(bpy-R)). This observation is in line with the increasing π-accepting properties of the diimine ligands bpy-R from R = NH_2 to R = ITC, and hence a decreasing energy level for the ^{3}MLCT (dπ(Ir) → π^*(bpy-R)) state.

Electrochemical Properties. The electrochemical properties of the cyclometalated iridium(III) diimine complexes are studied by cyclic voltammetry. The electrochemical data are listed in Table 3. The cyclic voltammograms of most of the complexes display an oxidation couple at potential between ca. +1.09 and +1.31 V vs SCE. With reference to previous electrochemical studies on related complexes,[4c,d,5b,e,f,9a,13b,15a,c] these couples are assigned to metal-centered Ir(IV/III) oxidation. However, the reversibility of these oxidation couples for the amine complexes is lower than that of their isothiocyanate and iodoacetamide analogues. Most of the phen-NH_2 complexes actually show irreversible oxidation waves with a sweep rate between 0.01 and 5 V s^{-1}. The irreversibility of this oxidation wave suggests the involvement of the coordinated phen-NH_2 ligand in the oxidation process.[19] Interestingly, irreversible oxidation waves have also been observed for some luminescent cyclometalated iridium(III) diimine complexes, whose HOMOs have been identified to have a high degree of σ(Ir−C) bonding character.[5e,i,7] The emission of these complexes has been assigned to a triplet σ-bond-to-ligand charge-transfer ^{3}SBLCT (σ(Ir−C) → π^*(diimine)) excited state. However, such an assignment for the phen-NH_2 complexes in this work is not justified, in view of the absence of a substantial blue-shift in the emission maxima upon cooling of these complexes to 77 K (Table 2), as a large blue-shift is commonly observed for iridium(III) SBLCT emitters.

On the other hand, the bpy-NH_2 and phen-NH_2 complexes exhibit the first reduction couples at ca. −1.60 and −1.45 V vs SCE, respectively (Table 3). These couples are associated with the reduction of the diimine ligands[4c,d,5a,b,e,f,i,7,9a,13,14,15a,c] instead of the cyclometalating ligands, as the latter are known to be reduced at lower potential.[4c,d,5a,b,e,f,i,7,9a,13,14,15a,c] The isothiocyanate and iodoacetamide complexes display the first reduction waves at ca. −1.2 and −1.0 V vs SCE, respectively (Table 3), attributed to the reduction of the diimine ligands. The occurrence of this reduction at less negative potential than that of the amine complexes is in agreement with the lower-lying π^* orbitals of the diimine ligands of the isothiocyanate and iodoacetamide complexes. However, since related cyclometalated iridium(III) complexes commonly show reversible diimine-based reduction,[4d,5a,b,e,f,i,7,13,14,15c] on the basis of the low reversibility of the reduction waves of the current complexes, we believe that these reduction processes are associated with the isothiocyanate and iodoacetamide moieties. In addition,

(19) (a) Ellis, C. D.; Margerum, L. D.; Murray, R. W.; Meyer, T. J. *Inorg. Chem.* **1983**, *22*, 1283. (b) Bachas, L. G.; Cullen, L.; Hutchins, R. S.; Scott, D. L. *J. Chem. Soc., Dalton Trans.* **1997**, 1571.

Table 4. Dye-to-Protein Ratios and Photophysical Data of Bioconjugates in Degassed 50 mM Tris-Cl Buffer at pH 7.4 at 298 K

conjugate	*D*/*P* ratio	λ_{em}/nm	Φ_{em}	τ_o/μs
$[Ir(ppy)_2(bpy\text{-}ITC)](PF_6)$-HSA	2.1	558	0.15	2.70 (26%), 0.53 (74%)
$[Ir(ppy)_2(phen\text{-}ITC)](PF_6)$-HSA	4.1	563	0.071	1.00 (30%), 0.18 (70%)
$[Ir(pq)_2(bpy\text{-}ITC)](PF_6)$-HSA	3.4	564, 602 sh	0.19	2.68 (57%), 0.36 (43%)
$[Ir(pq)_2(phen\text{-}ITC)](PF_6)$-HSA	1.4	559, 600 sh	0.11	2.85 (63%), 0.45 (37%)
$[Ir(ppy)_2(bpy\text{-}ITC)](PF_6)$-Av	0.43	560	0.043	0.81 (12%), 0.15 (88%)
$[Ir(ppy)_2(phen\text{-}ITC)](PF_6)$-Av	0.46	577	0.072	1.18 (8%), 0.34 (92%)
$[Ir(pq)_2(bpy\text{-}ITC)](PF_6)$-Av	0.16	560, 603 sh	0.19	3.13 (60%), 1.05 (40%)
$[Ir(pq)_2(phen\text{-}ITC)](PF_6)$-Av	0.22	560, 603 sh	0.16	3.91 (45%), 1.29 (55%)
$[Ir(mppz)_2(phen\text{-}IAA)](PF_6)$-HSA	1.33	563, 597 sh	0.050	0.68 (19%), 0.12 (81%)
$[Ir(mppz)_2(phen\text{-}IAA)](PF_6)$-GSH	1	594	0.014	0.067
$[Ir(mppz)_2(phen\text{-}IAA)](PF_6)$-Cys	1	588	0.005	0.065

Scheme 1. Reactions of (a) Isothiocyanate with a Primary Amine Group and (b) Iodoacetamide with a Sulfhydryl Group

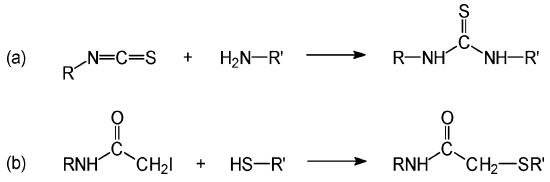

other quasireversible or irreversible waves are also observed for all the complexes at more negative potential, and some of these waves are highly distorted. It is likely that these waves are associated with the reduction of the diimine and cyclometalating ligands.

Biological Labeling Studies. Since the isothiocyanate moiety undergoes a facile addition reaction with the primary amine group to form a stable thiourea derivative (Scheme 1a), many organic compounds have been modified with an isothiocyanate group for covalent attachment to various biomolecules to give bioconjugates with new properties.[1,2,20] In view of this, we label protein molecules with some of the luminescent iridium(III) isothiocyanate complexes in this work. Four complexes $[Ir(N\text{-}C)_2(N\text{-}N)](PF_6)$ ($N\text{-}C^- = ppy^-$, pq^-; N-N = bpy-ITC, phen-ITC) are selected to label two proteins, human serum albumin (HSA) and avidin (Av). Under our reaction conditions, the dye-to-protein (*D*/*P*) ratios, determined by the Bradford method[21] and from the electronic absorption spectra of the free complexes and conjugates, vary between ca. 0.2 and 4 (Table 4). The *D*/*P* ratios are higher for the HSA conjugates than the Av conjugates, probably due to the fact that the number of lysine residues is higher for HSA than Av. The electronic absorption spectra of the conjugates show intense an absorption band at ca. 280 nm, attributed to both the protein molecule and the complex absorption, and other absorption shoulders in the visible region mainly due to the iridium(III) complexes. Upon photoexcitation, all the bioconjugates display intense and long-lived emission in aqueous buffer at 298 K (Table 4). The electronic absorption and emission spectra of the conjugate $[Ir(pq)_2(phen\text{-}ITC)](PF_6)$-Av are shown in Figure 4 as examples. Due to the phosphorescence nature of the emission, the Stokes shifts of the bioconjugates are large, leading to insignificant overlaps between the absorption and emission spectra. This is desirable because a large Stokes

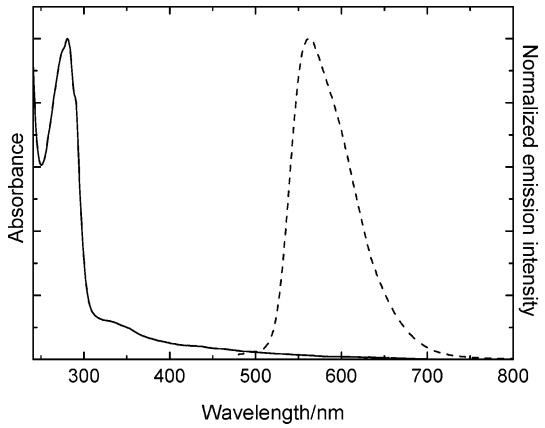

Figure 4. Electronic absorption (—) and emission (- - -) spectra of $[Ir(pq)_2(phen\text{-}ITC)](PF_6)$-Av in 50 mM Tris-Cl buffer at pH 7.4 at 298 K.

shift can avoid the self-quenching problem which is commonly encountered in the bioconjugates multiply labeled with organic fluorophores.[1,2] On the other hand, all the conjugates in the current study reveal biexponential emission decays, an observation that is not uncommon for biomolecules labeled with luminescent tags.[3,15] We tentatively assign the emission of the protein molecules labeled with the ppy^- complexes to an excited state of ^{3}MLCT ($d\pi(Ir) \rightarrow \pi^*$(diimine)) character. Meanwhile, the emission wavelengths of all the proteins labeled with $[Ir(pq)_2(N\text{-}N)](PF_6)$ (N-N = bpy-ITC, phen-ITC) are very similar, and some structural features are observed in the emission spectra. The emission quantum yields and lifetimes of these conjugates are also considerably higher and longer than those of their ppy^- counterparts. These observations suggest that the excited state of the pq^- bioconjugates possesses ^{3}IL ($\pi \rightarrow \pi^*$)(pq^-) character.

On the other hand, since the iodoacetamide group can react specifically with the sulfhydryl group to form a stable thioether (Scheme 1b),[1] we also label three sulfhydryl-containing biomolecules including HSA, glutathione (GSH), and cysteine (Cys) with the iodoacetamide complex $[Ir(mppz)_2(phen\text{-}IAA)](PF_6)$. All these three conjugates exhibit intense and long-lived yellow emission in Tris buffer at 298 K (Table 4). It is interesting to note that while the GSH and Cys conjugates show single-exponential emission decays, $[Ir(mppz)_2(phen\text{-}IAA)](PF_6)$-HSA displays a dual luminescence decay, suggestive of different microenvironments of the iridium labels on the HSA molecules. Also, the HSA conjugate emits at higher energy, with a higher emission quantum yield and a longer lifetime than the luminescent GSH and Cys molecules. These findings can be accounted

(20) (a) Jobbagy, A.; Kiraly, K. *Biochim. Biophys. Acta* **1966**, *124*, 166. (b) Strottmann, J. M.; Robinson, J. B., Jr.; Stellwagen, E. *Anal. Biochem*. **1983**, *132*, 334.
(21) Bradford, M. M. *Anal. Biochem.* **1976**, *72*, 248.

Scheme 2. Heterogeneous Competitive Assay for Digoxin[a]

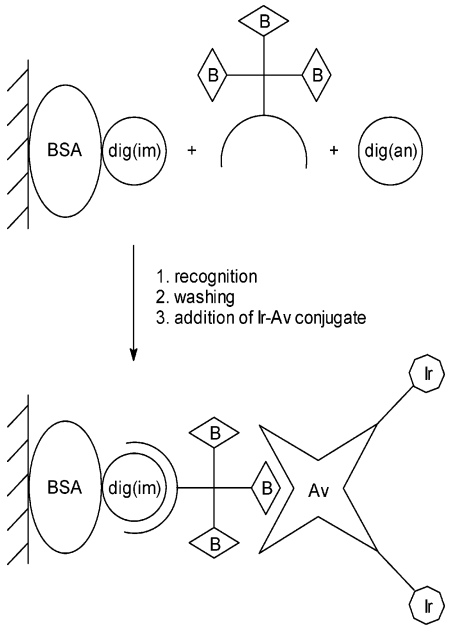

[a] BSA = immobilized bovine serum albumin as carrier protein, dig(im) = immobilized digoxin, B = biotin, dig(an) = digoxin analyte, Av = avidin, Ir = luminescent iridium labels.

for by the hydrophobicity of the serum albumin molecules, with reference to the photophysical data of the free complexes.

Digoxin Assays. Digoxin is a widely used cardiac glycoside for control of congestive heart failure and various disturbances of cardiac rhythm.[17] Homogeneous[22] and heterogeneous[23] immunoassays for digoxin have been developed to monitor the level of the drug in the sera. The design of heterogeneous immunoassays has relied on different tracers, including radionuclide-,[23a,b] enzyme-,[23c,d] chemiluminescence-,[23d] and lanthanide-based reagents.[23e,f] In addition, the use of ruthenium(II) diimine complexes as electrochemiluminescent labels in the development of digoxin immunoassays has also been investigated.[23g] In the present work, a heterogeneous immunoassay for digoxin using digoxin-coated microspheres, a biotinylated monoclonal anti-digoxin, and the luminescent conjugate $[Ir(pq)_2(phen\text{-}ITC)](PF)_6$-Av is studied. Bovine serum albumin (BSA) is used as a carrier protein to immobilize digoxin on carboxyl-modified microspheres.[24] The assay is based on the competition between the immobilized digoxin and free digoxin analyte for binding to the biotinylated anti-digoxin (Scheme 2). After the washing step, the biotinylated anti-digoxin captured on the solid phase is recognized by the luminescent avidin conjugate $[Ir(pq)_2(phen\text{-}ITC)](PF)_6$-Av. After incubation, the microspheres are removed, and the emission intensity of the supernatant is measured. A higher concentration of the digoxin analyte results in a lower number of immobilized biotinylated antibodies and a higher number of luminescent avidin molecules remaining in the supernatant and, hence, more intense emission. A similar heterogeneous assay has been developed to study the hybridization properties of an immobilized oligonucleotide with its complementary and fluorescently labeled counterpart present in bulk solution.[25]

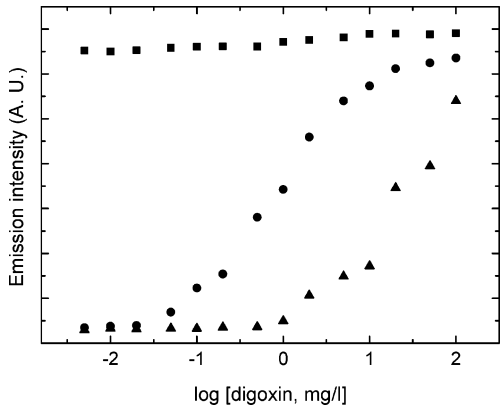

Figure 5. Standard curves for the heterogeneous competitive assays for digoxin using various masses of the digoxin-BSA conjugate. Mass of the digoxin-BSA conjugate for immobilization on microspheres: 2 (■), 20 (●), and 50 (▲) mg. All the other experimental conditions are the same as those of the optimized assay described in the Experimental Section.

We optimize the performance of the assays by changing various experimental parameters. First, the amount of digoxin-BSA conjugate immobilized on the microspheres is investigated. Increasing the amount of digoxin-BSA coating promotes nonspecific binding of the luminescent avidin conjugate to the solid phase.[23f] Although this nonspecific binding should be minimized, the amount of coated digoxin must be sufficient for the recognition by the biotinylated antibody (and then by the luminescent tracer molecules). In our optimization studies, the mass of the digoxin-BSA conjugate used for coating onto 2 mL (1:10 w/v) of carboxyl-modified microspheres suspension is varied. Standard curves obtained under the conditions for 2, 20, and 50 mg of the digoxin-BSA conjugate are shown in Figure 5 as examples. It is apparent that when 2 mg of the digoxin conjugate is used, the amount of immobilized digoxin is not sufficient for the recognition by the antibody and then by the luminescent avidin tracer, leading to the observations of high and indistinguishable emission intensity of the supernatant. When 50 mg of the digoxin-BSA conjugate is used, we do not observe any significant nonspecific binding. However, the sensitivity of the assay is lowered, and the lowest detectable concentration of digoxin analyte is ca. 1 mg/L (1.3×10^{-6} M), which is about 20 times more concentrated than that obtained under the optimum conditions (see details in a following paragraph). Experiments with more than 50 mg

(22) See, for example: (a) Drost, R. H.; Plomp, T. A.; Teunissen, A. J.; Maas, A. H. J.; Maes, R. A. A. *Clin. Chim. Acta* **1977**, *79*, 557. (b) Pinnaduwage, P.; Huang, L. *Clin. Chem.* **1988**, *34*, 268.

(23) See, for example: (a) Barbieri, U.; Gandolfi, C. *Clin. Chim. Acta* **1977**, *77*, 257. (b) Bergdähl, B.; Molin, L. *Clin. Biochem.* **1981**, *14*, 67. (c) Hinds, J. A.; Pincombe, C. F.; Morris, H.; Duffy, P. *Clin. Chem.* **1986**, *32*, 16. (d) Hubl, W.; Daxenbichler, G.; Meissner, D.; Thiele, H. J. *Clin. Chem.* **1988**, *34*, 2521. (e) Helsingius, P.; Hemmilä, I.; Lövgren, T. *Clin. Chem.* **1986**, *32*, 1767. (f) Papanastasiou-Diamandi, A.; Conway, K.; Diamandis, E. P. *J. Pharm. Sci.* **1989**, *78*, 617. (g) Blackburn, G. F.; Shah, H. P.; Kenten, J. H.; Leland, J.; Kamin, R. A.; Link, J.; Peterman, J.; Powell, M. J.; Shah, A.; Talley, D. B.; Tyagi, S. K.; Wilkins, E.; Wu, T.-G.; Massey, R. J. *Clin. Chem.* **1991**, *37*, 1534.

(24) Bulter, V. P.; Tse-Eng, D. *Methods in Enzymology*; Academic Press: San Diego, CA, 1982; Vol, 84, p 558.

(25) Stevens, P. W.; Henry, M. R.; Kelso, D. M. *Nucleic Acids Res.* **1999**, *27*, 1719.

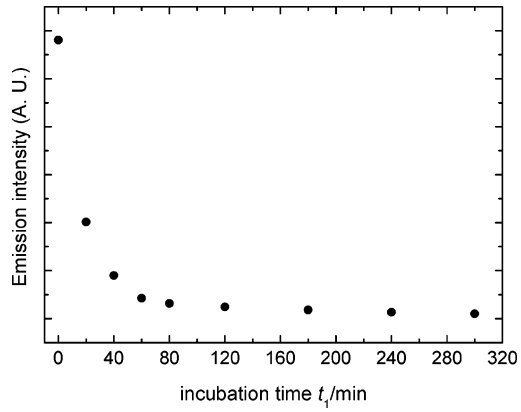

Figure 6. Plot of the emission intensity of the supernatant against the incubation time, t_1, for the binding of the biotinylated antibody to the immobilized digoxin. Free digoxin analytes are absent. All the other experimental conditions are the same as those of the optimized assay described in the Experimental Section.

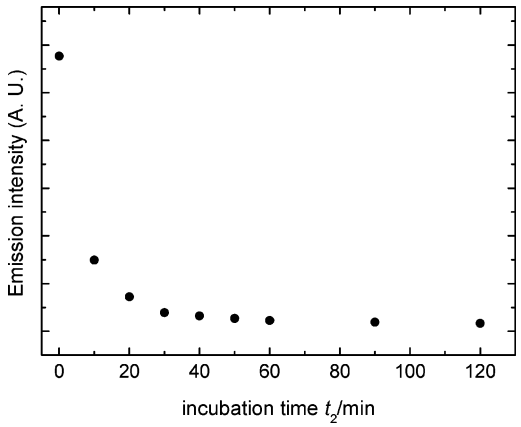

Figure 7. Plot of the emission intensity of the supernatant against the incubation time, t_2, for the binding of the luminescent iridium-avidin conjugate to the immobilized antibody. Free digoxin analytes are absent. All the other experimental conditions are the same as those of the optimized assay described in the Experimental Section.

of the digoxin-BSA conjugate are not attempted due to solubility reasons. After the immobilization of the digoxin-BSA conjugate, the coated surface is further blocked with BSA. We observe that unblocked microsphere samples often lead to nonreproducible results. This is likely to be a consequence of nonspecific binding of the antibody and/or the luminescent avidin reagent to the solid phase.

The concentration of the luminescent iridium-avidin conjugate is also varied to optimize the performance of the assays. When a high concentration (> 0.3 mM) is used, the emission intensities of the samples are generally very high and indiscernible from each other (data not shown). However, if the concentration of the luminescent avidin conjugate is below ca. 0.001 mM, the emission intensity of the supernatant is too low within the analyte concentration range of interest. The optimum concentration of the luminescent iridium-avidin conjugate is determined to be 0.03 mM with respect to avidin.

The minimum incubation times required for the reactions of (i) the antibody and the immobilized digoxin (t_1), and (ii) the luminescent iridium-avidin conjugate and the immobilized biotinylated antibody (t_2) to reach equilibria are evaluated by simple kinetics studies at room temperature. Incubation times from 0 to 300 min for t_1 and from 0 to 120 min for t_2 are investigated, and no digoxin analytes are used in these experiments. The longer the incubation times, the more luminescent tracers are eventually bound to the microspheres, resulting in reduced emission intensity of the supernatant. The relationships between the emission intensity of the supernatant containing the unbound luminescent iridium-avidin conjugate and the incubation times t_1 and t_2 are illustrated in Figures 6 and 7, respectively. We notice that constant emission intensity is reached in ca. 60 min (t_1) for the binding of the antibody, to the solid phase, and in ca. 30 min (t_2) for the recognition of the antibody by the luminescent iridium-avidin conjugate. These two incubation times are therefore employed in our immunoassay experiments.

After the optimizations, the emission intensity of the supernatant is measured over a concentration range of the digoxin analyte from 0.005 to 100 mg/L (6.4×10^{-9} to 1.3×10^{-4} M) (Figure 8). The lowest concentration of digoxin analyte that gives a meaningful signal over background is ca. 0.05 mg/L (6.4×10^{-8} M). The value is higher than the limits of detection in other digoxin assays.[23e−g] The concentration range of digoxin that can be measured is between ca. 0.05 and 20 mg/L (6.4×10^{-8} and 2.6×10^{-5} M). We expect that the detection limit of the assay can be further improved by using other approaches, such as incorporating iridium-avidin conjugates into other larger biomolecules to form luminescent macromolecular species which is then used as the detection agent. Nevertheless, utilization of luminescent iridium(III) diimine complexes as labeling reagents in the development of related assays for other biological molecules such as proteins, nucleic acids, and toxin molecules is very promising.

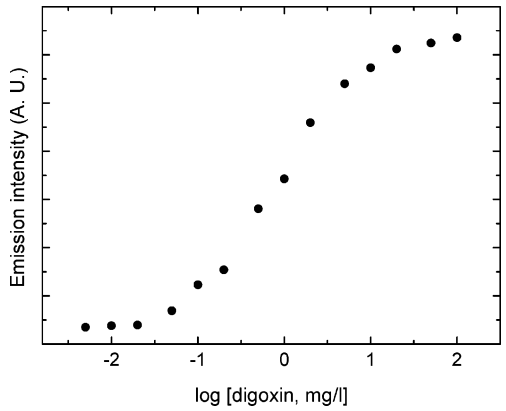

Figure 8. Standard curve for the optimized heterogeneous competitive assay for digoxin using digoxin-modified microspheres, biotinylated anti-digoxin, and the conjugate $[Ir(pq)_2(phen\text{-}ITC)](PF_6)$-Av. The emission intensity of the supernatant is plotted against the concentrations of digoxin analytes. The conditions of the assay are described in the Experimental Section.

Conclusion

A family of luminescent cyclometalated iridium(III) polypyridine complexes is synthesized and characterized, and their photophysical and electrochemical properties are in-

vestigated. The nature of the excited states of these luminescent complexes is identified on the basis of the photophysical and electrochemical data. Some of these complexes contain amine-specific isothiocyanate and sulfhydryl-specific iodoacetamide groups, and they are used to label various biological molecules including Cys, GSH, HSA, and Av. The luminescent conjugates are isolated and their photophysical properties developed. A heterogeneous assay for digoxin is also studied using one of the luminescent iridium-avidin conjugates. We anticipate that, by using other functional ligands, novel iridium(III) polypyridine complexes with rich desirable photochemical and photophysical properties can be produced, and the exploitation of these complexes as new biological labels and probes can be realized.

Experimental Section

Materials and Synthesis. All solvents were of analytical reagent grade and purified according to standard procedures. The following chemicals were used without further purification: $IrCl_3 \cdot 3H_2O$ (Acros), Hppy (Aldrich), Hmppy (Aldrich), Hmppz (Acros), Hbzq (Acros), Hpq (Acros), 2,2′-bipyridine (Acros), *N*,*N*′-dicyclohexylcarbodiimide (Acros), iodoacetic acid (Acros), potassium hexafluorophosphate (Acros), thiophosgene (Aldrich), iodoacetyl chloride (Lancaster), calcium carbonate (RDH), polyoxyethylenesorbitan monolaurate (Tween 20) (Alrich), sodium azide (Sigma), Cys (Sigma), GSH (Sigma), digoxin (Sigma), sodium periodate (Acros), sodium borohydride (Acros), 1-(3-dimethylaminopropyl)-3-ethylcarbodiimide hydrochloride (EDC) (Acros), and monoclonal anti-digoxin biotin conjugate (Sigma). BSA, HSA, and Av were from Calbiochem and were used as received. Carboxyl-modified microspheres (0.43 μm) were from the Bangs Laboratories. The digoxin-BSA conjugate was prepared by a reported method,[24] and the digoxin/BSA ratio was determined to be 4.2 for our sample. For the bioassays, the wash solution was NaCl solution (9 g/L) containing Tween 20 (0.5 mL/L). The blocking buffer was potassium phosphate buffer (50 mM, pH 7.4) containing NaCl (9 g/L), BSA (10 g/L), and Tween 20 (1 mL/L). The assay buffer was Tris-Cl buffer (50 mM, pH 7.4) containing BSA (10 g/L), NaCl (9 g/L), and sodium azide (0.5 g/L). The stock antibody solution (4.3 mg/mL) was dialyzed against NaCl solution (9 g/L) at 4 °C. In the assays, this solution was diluted with the assay buffer to a concentration of 430 mg/L.

$[Ir(N\text{-}C)_2(N\text{-}N)](PF_6)$ (N-N = bpy-NH_2 or phen-NH_2). A mixture of $[Ir_2(N\text{-}C)_4Cl_2]$[4b] (0.20 mmol) and bpy-NH_2 [26] or phen-NH_2 [27] (0.40 mmol) in 30 mL methanol/dichloromethane (1:1 v/v) was refluxed under an inert atmosphere of nitrogen in the dark for 4 h. The orange-red to yellow solution was then cooled to room temperature, and KPF_6 (74 mg, 0.40 mmol) was added to the solution. The mixture was then evaporated to dryness, and the solid was dissolved in dichloromethane and purified by column chromatography on silica gel. The desired product was eluted with dichloromethane/acetone (1:1 v/v). Recrystallization from acetone/diethyl ether afforded the complex as orange-red to yellow crystals.

$[Ir(N\text{-}C)_2(N\text{-}N)](PF_6)$ (N-N = bpy-ITC or phen-ITC). A mixture of the amine complex (0.10 mmol), thiophosgene (22 μL, 0.30 mmol), and calcium carbonate (60 mg, 0.60 mmol) in 10 mL acetone was stirred under an inert atmosphere of nitrogen at room temperature for 3 h. The solution was filtered and then evaporated to dryness. The brown to orange-yellow solid was washed with petroleum ether. Recrystallization from acetone/diethyl ether afforded the complex as orange-red to yellow crystals.

$[Ir(N\text{-}C)_2(bpy\text{-}IAA)](PF_6)$. A mixture of $[Ir(N\text{-}C)_2(bpy\text{-}NH_2)](PF_6)$ (0.10 mmol), ICH_2COCl (80 μL), and $CaCO_3$ (150 mg, 1.50 mmol) in 15 mL dichloromethane was stirred under an inert atmosphere of nitrogen at room temperature for 2 days. The solution was filtered and then evaporated to dryness. The brown solid was washed with diethyl ether/petroleum ether (1:1 v/v) to remove excess ICH_2COCl. Recrystallization from dichloromethane/petroleum ether afforded the complex as brown to orange-yellow crystals.

$[Ir(N\text{-}C)_2(phen\text{-}IAA)](PF_6)$. A mixture of $[Ir(N\text{-}C)_2(phen\text{-}NH_2)](PF_6)$ (0.10 mmol) and iodoacetic anhydride[28] (177 mg, 0.50 mmol) in 10 mL acetonitrile was stirred under an inert atmosphere of nitrogen at room temperature for 24 h. The solution was then evaporated to dryness. The orange solid was washed with diethyl ether to remove ICH_2COOH and excess $(ICH_2CO)_2O$. Recrystallization from acetonitrile/diethyl ether afforded the complex as orange to yellow crystals.

Characterization data of all the complexes are included in the Supporting Information.

Physical Measurements and Instrumentation. Equipment for characterization and photophysical and electrochemical studies has been described previously.[15] Luminescence quantum yields were measured by the optical dilute method[29] using an aerated aqueous solution of $[Ru(bpy)_3]Cl_2$ ($\Phi = 0.028$)[30] as the standard solution.

X-ray Structural Analysis for $[Ir(mppz)_2(bpy\text{-}NH_2)](PF_6)$. Single crystals of the complex suitable for X-ray crystallographic studies were obtained by slow diffusion of diethyl ether vapor into a concentrated dichloromethane solution of the complex. A crystal of dimensions $0.7 \times 0.3 \times 0.25$ mm^3 mounted in a glass capillary was used for data collection at 28 °C on a MAR diffractometer with a 300 mm image plate detector using graphite monochromatized Mo Kα radiation ($\lambda = 0.710\ 73$ Å). Data collection was made with 3° oscillation step of φ, 600 s exposure time, and scanner distance at 120 mm. Images (60) were collected. The images were interpreted and intensities integrated using the program DENZO.[31] The structure was solved by direct methods employing the SHELXS-97 program[32] on a PC. Iridium, phosphorus, and many non-hydrogen atoms were located according to the direct methods. The positions of other non-hydrogen atoms were found after successful refinement by full-matrix least-squares using the program SHELXL-97[32] on a PC. In the asymmetric unit, CH_2Cl_2, H_2O, and PF_6^- anion were located with half occupancy, respectively. The amine group of the bpy-NH_2 ligand is disordered, due to the flipping of the ligand. One crystallographic asymmetric unit consists of half of formula unit, including half anion and half dichloromethane and half water solvent molecules. In the final stage of least-squares refinement, all non-hydrogen atoms were refined anisotropically. Hydrogen atoms were generated by SHELXL-97. The positions of the hydrogen atoms were calculated on the basis of riding mode with thermal parameters equal to 1.2 times that of the associated C atoms, and they participated in the calculation of final *R*-indices.

(26) Jones, R. A.; Roney, B. D.; Sasse, W. H. F.; Wade, K. O. *J. Chem. Soc. B* **1967**, 106.
(27) Del Guerzo, A.; Demeunynck, M.; Lhomme, J.; Kirsch-De Mesmaeker, A. *Inorg. Chem. Commun.* **1998**, *1*, 339.
(28) Takalo, H.; Mukkala, V.-M.; Mikola, H.; Liitti, P.; Hemmilä, I. *Bioconjugate Chem.* **1994**, *5*, 278.
(29) Demas, J. N.; Crosby, G. A. *J. Phys. Chem.* **1971**, *75*, 991.
(30) Nakamaru, K. *Bull. Chem. Soc. Jpn.* **1982**, *55*, 2697.
(31) DENZO: Otwinowski, Z.; Minor, W. *Methods in Enzymology*; Academic Press: San Diego, CA, 1997; Vol, 276, p 307.
(32) SHELXS-97 and SHELXL-97: Sheldrick, G. M. *Programs for Crystal Structure Analysis (Release 97-2)*; University of Göttingen: Göttingen, Germany.

Table 5. Crystal Data and Summary of Data Collection and Refinement for $[Ir(mppz)_2(bpy\text{-}NH_2)](PF_6)$

formula	$C_{31}H_{30}Cl_2F_6IrN_7OP$
fw	924.69
crystal size (mm^3)	$0.7 \times 0.3 \times 0.25$ mm^3
T (K)	301
cryst syst	orthorhombic
space group	*Cmca*
a (Å)	22.772(5)
b (Å)	18.227(4)
c (Å)	17.728(4)
V (Å^3)	7358(3)
Z	8
ρ_{calcd} (g cm^{-3})	1.669
μ (mm^{-1})	3.884
F(000)	3624
θ range (deg)	2.71−25.54
oscillation (deg)	3
no. images collected	60
distance (mm)	120
exposure time (s)	360
index ranges	$-27 \le h \le 27$ $-20 \le k \le 20$ $-20 \le l \le 20$
no. data collected	22424
R_{int} [a]	0.0419
no. unique data/restraints/params	3324/0/239
GOF on F^2 [b]	1.048
R1, wR2 ($I > 2\sigma(I)$)[c]	0.0526, 0.1567
R1, wR2 (all data)	0.0781, 0.1682
largest diff. peak/hole (e Å^{-3})	0.910, −1.211

[a] $R_{int} = \sum|F_o^2 - F_o^2(\text{mean})|/\sum[F_o^2]$. [b] GOF $= \{\sum[w(F_o^2 - F_c^2)^2]/(n - p)\}^{1/2}$, where n is the number of reflections and p is the total number of parameters refined. The weighting scheme is $w = 1/[\sigma^2(F_o^2) + (aP)^2 + bP]$, where P is $[2F_o^2 + \max(F_o^2,0)]/3$, $a = 0.0929$, and $b = 25.004$. [c] R1 $= \sum||F_o| - |F_c||/\sum|F_o|$, wR2 $= \{\sum[w(F_o^2 - F_c^2)^2]/\sum[w(F_o^2)^2]\}^{1/2}$.

Crystal data and a summary of data collection and refinement details are given in Table 5.

Labeling of HSA and Av with $[Ir(N\text{-}C)_2(N\text{-}N)](PF_6)$ (N-C$^-$ = ppy$^-$, pq$^-$; N-N = bpy-ITC, phen-ITC). The iridium(III) isothiocyanate complex (0.76 μmol) dissolved in anhydrous DMSO (20 μL) was added to HSA or Av (10 mg, 0.15 μmol) dissolved in 180 μL 50 mM carbonate buffer, pH 9.7. The suspension was stirred for 12 h in the dark at room temperature. The solid residue was removed by centrifugation. The supernatant was then diluted to 1.0 mL with 50 mM Tris-Cl, pH 7.4, and loaded onto a PD-10 column (Pharmacia) that had been equilibrated with the same buffer. The first band with strong orange-yellow photoluminescence was collected. The conjugates $[Ir(ppy)_2(bpy\text{-}ITC)](PF_6)$-HSA, $[Ir(ppy)_2(phen\text{-}ITC)](PF_6)$-HSA, $[Ir(pq)_2(bpy\text{-}ITC)](PF_6)$-HSA, $[Ir(pq)_2(phen\text{-}ITC)](PF_6)$-HSA, $[Ir(ppy)_2(bpy\text{-}ITC)](PF_6)$-Av, $[Ir(ppy)_2(phen\text{-}ITC)](PF_6)$-Av, $[Ir(pq)_2(bpy\text{-}ITC)](PF_6)$-Av, and $[Ir(pq)_2(phen\text{-}ITC)](PF_6)$-Av were then concentrated with a YM-30 centricon (Amicon) and then further purified by size-exclusion HPLC.

Labeling of Cys and GSH with $[Ir(mppz)_2(phen\text{-}IAA)](PF_6)$. $[Ir(mppz)_2(phen\text{-}IAA)](PF)_6$ (9.8 mg, 9.6 μmol) dissolved in anhydrous DMSO (100 μL) was added to Cys (1.1 mg, 8.8 μmol) or GSH (2.7 mg, 8.8 μmol) dissolved in 100 μL 50 mM phosphate buffer, pH 7.4. The mixture was stirred in the dark at room temperature for 24 h. The precipitate was removed by centrifugation. The excess labels were removed by washing the supernatant with ethyl acetate (200 μL × 10), and the conjugates were further purified by reversed-phase HPLC. Positive-ion ESI-MS ion clusters were at m/z 863 for $\{[Ir(mppz)_2(phen\text{-}IAA)](PF_6)\text{-}Cys\}^+$ and at m/z 1047 for $\{[Ir(mppz)_2(phen\text{-}IAA)](PF_6)\text{-}GSH\}^+$.

Coating of Carboxyl-Modified Microspheres with Digoxin-BSA Conjugate. A suspension (2 mL) of carboxyl-modified microspheres (diameter 0.43 μm) in deionized water (1:10 w/v) was centrifuged for 30 min (13 000 rpm). The water was then removed carefully using a micropipet. The digoxin-BSA conjugate[24] (20 mg) and EDC (0.06 mg, 0.30 μmol) dissolved in 50 mM carbonate buffer, pH 9.7 (2 mL), were added to the microsphere pellet. The suspension was stirred at room temperature for 48 h. Then, the modified microspheres were collected by centrifugation, and the supernatant was removed. After the coating, the microspheres were washed three times with the wash solution and then blocked for 24 h at room temperature with the blocking buffer (2 mL). Finally, the blocked microspheres were washed with the wash solution twice and then stored in the assay buffer (2 mL) at 4 °C.

Heterogeneous Competitive Immunoassay for Digoxin. Digoxin analyte solution (20 μL) was mixed with the coated microspheres suspension (10 μL) in the assay buffer, and then, diluted biotinylated monoclonal anti-digoxin solution (20 μL, 200 mg/L) was added. The final concentration of the digoxin analytes in the assay mixtures ranged from 0.005 to 100 mg/L (6.4×10^{-9} to 1.3×10^{-4} M). The suspension was then incubated at room temperature for 1 h with continuous stirring. The microspheres were then collected by centrifugation and washed four times with the wash solution. Afterward, diluted $[Ir(pq)_2(phen\text{-}ITC)](PF_6)$-Av (50 μL, 0.03 mM, relative to Av, $D/P = 1.4$) was added to the mixture. The mixture was incubated at room temperature for 30 min, and the supernatant was isolated by centrifugation. The luminescence intensity of the supernatant was measured using a 3 mm fluorescence cuvette.

Acknowledgment. We thank the Hong Kong Research Grants Council (Project No. CityU1113/02P) and the City University of Hong Kong (Project No. 7100272) for financial support. C.-K.C. and K.H.-K.T. acknowledge the receipt of a postgraduate studentship and a Research Tuition Scholarship, both administered by the City University of Hong Kong. We are grateful to Professor Vivian W.-W. Yam of The University of Hong Kong for access to the equipment for photophysical measurements.

Supporting Information Available: Characterization and electronic absorption spectral data of all the iridium(III) complexes and X-ray data (CIF) of $[Ir(mppz)_2(bpy\text{-}NH_2)](PF_6)$. This material is available free of charge via the Internet at http://pubs.acs.org.

IC0346984